Available online at www.sciencedirect.com

ScienceDirect

IFAC Papers Online CONFERENCE PAPER ARCHIVE

IFAC-PapersOnLine 49-1 (2016) 712–717

Design and Simulation of Autopilot Control System for Stratospheric Airship

Ramesh Hun*, Anshul Tiwari**, and Nandan Kumar Sinha***

*Research scholar and Corresponding author
(e-mail: ramesh.iitm14@ gmail.com).
**Research scholar: tiwariskybuster@gmail.com
*** Professor, Senior Member AIAA, nandan@ae.iitm.ac.in
Department of Aerospace Engineering, IIT Madras, Chennai-36, INDIA.

Abstract: Design of an effective autopilot control system for Lighter-Than-Air (LTAs) vehicles, especially for stratospheric airship is crucial. A Stratospheric Airship Platform (SAP) is required to perform various autopilot control actions to satisfy the mission requirements. The main control actions are holding altitude, velocity, pitch and bank angles at desired operating conditions, which are also important for autonomous navigation and guidance purposes. Proportional-Integral-Derivative (PID) is one of the traditional control algorithms and plays key role in the achievement of given requirements. In this paper, a successive loop closure design method has been implemented and compared with respect to the autopilot control actions mentioned above. Successive loop of PI controller is used to emphasize more on steady state behavior rather than transient behavior of the autopilots. Graphical User Interface (GUI) is developed in SISO architecture tool in MATLAB® for the simulation of different autopilots. Simulation results show that designed autopilots are optimal in terms of transient and steady state specifications.

© 2016, IFAC (International Federation of Automatic Control) Hosting by Elsevier Ltd. All rights reserved.

Keywords: Autopilot, Stratospheric Airship Platform, Successive Loop Closure, Graphical User Interface

1. INTRODUCTION

After their first stint around wold war II, airships are being re-considered as potential LTA systems for applications such as high altitude surveillance thus providing an alternative for Low-Earth observation satellites. To operate at such high altitudes as stratosphere in station-keeping mode strong on-board autopilot systems are mandatory. Several autopilots have been proposed in literature for different configurations of airships. A velocity hold autopilot for Tri-Turbofan remotely controlled-low altitude airship was proposed in Ref. [2007]. López Fernández, J.et al. [2009] designed and developed fuzzy logic based controller for low cost commercial indoor blimp. They observed significant difference in performance of the controller in in-door (no wind) and out-door (windy) conditions. Kadota et al. [2004] developed vision based positioning algorithm with the use of PID controller to control blimp altitude and horizontal movement in the in-door environment. Lee and co-authors [2005] designed an Automatic Flight Control System (AFCS) based on PID tuning using root locus for a 50m airship. Zeigler and Nichols [1942] method used by them is only suitable for systems having a pair of eigenvalues crossing imaginary axis. Another restriction of using this method is that it works for fixed performance specifications instead of desired specifications.

PID control technique is popular for its simplicity, can handle desired multiple transient specifications simultaneously and is easy to implement. Therefore, it is preferred to use PID based techniques for a first cut design of autopilot systems. The other reason being that market available controllers, for example Arduino controllers provides in-built library for developing tuning based PID laws. The mathematical model for the stratospheric airship developed in-house [Vikas, R et al. 2015] has been used in this work. ASISO architecture based successive loop closure technique for the design of different autopilots for the stratospheric airship model is implemented in MATLAB®. This method also facilitates user based manual tuning to meet the certain specification requirement.

This paper is organized as follows. Section 2 presents the mathematical model of airship briefly. Section 3 presents design strategy of different autopilot control system along with stability analysis of designed autopilots. Section 4 concludes and summarizes this work.

2. MATHEMATICAL MODEL

2.1 Non-linear Mathematical Model

An airship is a buoyancy based vehicle with six degrees of freedom in motion. Governing equations of airship motion are slightly different than that of conventional rigid body airplanes with most significant difference being terms including added mass and inertial effects [1927]. The complete set of nonlinear equations in compact form can be represented as,

$$\boldsymbol{M}\dot{\underline{X}} = \underline{\boldsymbol{F_d}}(u,v,w,p,q,r) + \underline{\boldsymbol{A}}(u,v,w,p,q,r) + \underline{\boldsymbol{G}} + \underline{\boldsymbol{P}} \quad (1)$$

Where, $\boldsymbol{M}$ is a mass matrix representing the apparent mass and apparent inertia as well as apparent product of inertia terms. $\underline{X}$ represents vector of state variables of airship consisting of three linear velocity components (u, v, w) and three angular velocity components (p, q, r). Vector $\underline{\boldsymbol{F_d}}$ represents dynamic terms associated with linear and angular velocities. Vector $\underline{\boldsymbol{A}}$ is a column matrix consisting of the aerodynamics force and moment terms. Vector $\underline{\boldsymbol{G}}$ contains the terms related to

2405-8963 © 2016, IFAC (International Federation of Automatic Control) Hosting by Elsevier Ltd. All rights reserved.
Peer review under responsibility of International Federation of Automatic Control.
10.1016/j.ifacol.2016.03.140

gravitational and bouncy forces and moments. Vector $\underline{\boldsymbol{P}}$ contains the terms associated with propulsive forces and moments.

2.2 Linearization of Equation of Motion

The six degree of freedom nonlinear equations of motion in equation (1) describe fully coupled dynamics of airship. To simulate the PID control algorithm, the non-linear equations are linearized about a particular operating condition using small perturbation technique [Khoury, G.A. et al., 2004]. Here, a level flight condition is chosen as the operating condition. The linearized equations of motion can be represented by standard state space form as below,

$$\Delta\underline{\dot{X}} = A\Delta\underline{X} + B\Delta\underline{U} \tag{2}$$

Where $\underline{U}$ indicates control parameters which are used for motion control of airship. $A = \left(\frac{\partial F}{\partial X}\right)_{(X^*,U^*)}$ is the system matrix and $B = \left(\frac{\partial F}{\partial U}\right)_{(X^*,U^*)}$ is the control matrix. The transfer function of each state variable w.r.t the control inputs can be obtained as,

$$\frac{\underline{X}(s)}{\underline{U}(s)} = \frac{Adj[sI-A]}{|sI-A|}B \tag{3}$$

Where, the solutions of the characteristic equation $|sI - A| = 0$ determine the stability of the system. The linearized equations of motion obtained from equation (2) can be decoupled in two parts namely longitudinal and lateral equations.

1. Longitudinal dynamics

The linearized longitudinal equations of motion in the state space form can be written as,

$$m_l\underline{\dot{X}_l} = a_l\underline{X_l} + b_l\underline{U_l} \tag{4}$$

Where,

$$m_l = \begin{bmatrix} m_x & 0 & ma_z - X_{\dot{q}} & 0 \\ 0 & m_z & -(ma_x + Z_{\dot{q}}) & 0 \\ ma_z - M_{\dot{u}} & -(ma_x + M_{\dot{w}}) & J_y & 0 \\ 0 & 0 & 0 & 1 \end{bmatrix}$$

$$a_l = \begin{bmatrix} X_u & X_w & X_q - m_zW_e & -(mg - B)\cos\theta_e \\ Z_u & Z_w & Z_q + m_xU_e & -(mg - B)\sin\theta_e \\ M_u & M_w & M_q - ma_xU_e - ma_zW_e & m' \\ 0 & 0 & 1 & 0 \end{bmatrix}$$

Where,

$$m' = -\{(mga_z + Bb_z)\cos\theta_e - (mga_x + Bb_x)\sin\theta_e\}$$

$$b_l = \begin{bmatrix} X_\delta & X_t \\ Z_\delta & 0 \\ M_\delta & M_t \\ 0 & 0 \end{bmatrix}$$

$X_l^T = [u\ w\ q\ \theta]$, $U_l^T = [\delta_e\ \delta_t]$

Equation (4) is pre-multiplied by m_l^{-1} to transform it into the standard state space form,

$$\underline{\dot{X}_l} = A_l\underline{X_l} + B_l\underline{U_l} \tag{5}$$

Where $A_l = m_l^{-1}a_l$ and $B_l = m_l^{-1}b_l$

The complete set of transfer functions for the longitudinal states is obtained from equation (5) and are listed in table 1. Here, elevator is chosen as the input control parameter.

Table 1. Longitudinal states transfer function

$\frac{o/p}{i/p}$	Transfer Function
$\frac{u(s)}{\delta_e}$	$\frac{0.0022k(s+0.06931)(s^2+0.4852s+0.1492)}{(s+0.04833)(s+0.004352)(s^2+0.06012s+0.01331)}$
$\frac{w(s)}{\delta_e}$	$\frac{-0.1066k(s+0.0004367)(s^2+0.114s+0.0155)}{(s+0.04833)(s+0.004352)(s^2+0.06012s+0.01331)}$
$\frac{q(s)}{\delta_e}$	$\frac{-0.001228ks(s+0.0875)(s+0.0004435)}{(s+0.04833)(s+0.004352)(s^2+0.06012s+0.01331)}$
$\frac{\theta(s)}{\delta_e}$	$\frac{-0.00122k(s+0.0875)(s+0.004435)}{(s+0.04833)(s+0.004352)(s^2+0.06012s+0.01331)}$

2. Lateral-directional dynamics

The linearized lateral-directional equations of motion in the state space form can be written as,

$$m_{lt}\underline{\dot{X}_{lt}} = a_{lt}\underline{X_{lt}} + b_{lt}\underline{U_{lt}} \tag{6}$$

Where,

$$m_{lt} = \begin{bmatrix} m_y & -(ma_z + Y_{\dot{p}}) & ma_x - Y_{\dot{r}} & 0 \\ -(ma_z + L_{\dot{v}}) & J_x & -J_{xz} & 0 \\ ma_x - N_{\dot{v}} & -J_{xz} & J_z & 0 \\ 0 & 0 & 0 & 1 \end{bmatrix}$$

$$a_{lt} = \begin{bmatrix} Y_{\dot{v}} & Y_p + m_zW_e & Y_r - m_xU_e & (mg - B)\cos\theta_e \\ L_{\dot{v}} & L_p - ma_zW_e & L_r + ma_zU_e & -(mga_z + Bb_z)\cos\theta_e \\ N_{\dot{v}} & N_p + ma_xW_e & N_r - ma_xU_e & (mga_x + Bb_x)\cos\theta_e \\ 0 & 1 & 0 & 0 \end{bmatrix}$$

$$b_{lt} = \begin{bmatrix} Y_{\delta_r} \\ 0 \\ N_{\delta_r} \\ 0 \end{bmatrix}$$

$X_{lt}^T = [v\ p\ r\ \phi]$, $U_{lt}^T = [\delta_r\ \delta_a]$

In order to transform it in the standard state space form, equation (6) is pre-multiplied by m_{lt}^{-1} as earlier,

$$\underline{\dot{X}_{lt}} = A_{lt}\underline{X_{lt}} + B_{lt}\underline{U_{lt}} \tag{7}$$

Where $A_{lt} = m_{lt}^{-1}a_{lt}$ and $B_{lt} = m_{lt}^{-1}b_{lt}$.

The complete set of transfer functions obtained using equation (7) are listed in table 2 given below. The transfer functions of lateral states are derived with rudder as the control parameter.

Table 2. Transfer functions of lateral states

$\frac{o/p}{i/p}$	Transfer Function
$\frac{v(s)}{\delta_r}$	$\frac{-0.00031k(s-2.014)(s^2+0.227s+0.3969)}{(s+0.07923)(s+0.008027)(s^2+0.02244s+0.2657)}$
$\frac{p(s)}{\delta_r}$	$\frac{-0.0000346k\,s(s+1.236)(s+0.01386)}{(s+0.07923)(s+0.008027)(s^2+0.02244s+0.2657)}$
$\frac{r(s)}{\delta_r}$	$\frac{-0.00025k(s+0.008691)(s^2+0.2353s+0.2674)}{(s+0.07923)(s+0.008027)(s^2+0.02244s+0.2657)}$
$\frac{\phi(s)}{\delta_r}$	$\frac{-0.0000346k\,(s+1.236)(s+0.01386)}{(s+0.07923)(s+0.008027)(s^2+0.02244s+0.2657)}$

From the transfer functions, it is evident that system is stable in the open loop. To analyse the closed loop system stability, a gain parameter k is introduced in each of the transfer functions.The system will be stable for only some specific values of k. This range of k is very important while designing an autopilot system (How, J.P. et al., 2015). The values of k for which closed loop system is stable is obtained using root locus method and are given in tables 3 and 4.

Table 3. Closed loop stability of longitudinal states

Gain	Longitudinal States Transfer Function			
	$\frac{u(s)}{\delta_e}$	$\frac{w(s)}{\delta_e}$	$\frac{q(s)}{\delta_e}$	$\frac{\theta(s)}{\delta_e}$
k	$0<k\leq 0.1$	$0<k\leq 0.38$	$0<k\leq 42.5$	$0<k\leq 5.87$

Table 4. Closed loop stability of lateral state

Gain	Lateral States Transfer Function			
	$\frac{v(s)}{\delta_r}$	$\frac{p(s)}{\delta_r}$	$\frac{r(s)}{\delta_r}$	$\frac{\phi(s)}{\delta_r}$
k	$0<k\leq 42.4$	$0<k\leq 482$	$0<k\leq 290$	$0<k\leq 284$

Another basic criteria that any system must follow to have a feasible control design is that it should satisfy the controllability condition. Before proceeding into further steps, the controllability condition must be checked and satisfied. The controllability conditions for the longitudinal and lateral motions are given below.

Controllability test for longitudinal motions:

The controllability matrix for longitudinal dynamics of the airship model is defined as,

$$Q_{lC} = [B_l \vdots A_l B_l \vdots A_l^2 B_l \vdots A_l^3 B_l]$$

Which is of rank 4, therefore it is concluded that longitudinal motions are completely controllable.

Controllability test for lateral-directional motions:

The controllability matrix for lateral-directional dynamics is defined as

$$Q_{ltC} = [B_{lt} \vdots A_{lt} B_{lt} \vdots A_{lt}^2 B_{lt} \vdots A_{lt}^3 B_{lt}]$$

Which is of rank 4, therefore lateral motions are completely controllable.

3. AUTOPILOT DESIGN

Strategy for the design of autopilots in this work emphasizes more on steady state error rather than transient response. However due consideration is also given to avoid undesired transient response. Since we are dealing with decoupled set of equations for both lateral and longitudinal motions, the successive loop closure method can be used here for the PID controller design [Beard et al., 2012]. Derivative term from PID law is dropped in this analysis because of effect of derivative on measurement variable (*MV*) which is given by, $\frac{d(e(t))}{dt} = \frac{d(SP-MV)}{dt} = -\frac{d(MV)}{dt}$ for a constant *SP* (set point). Therefore, derivative controller amplifies the measurement noise at high frequency which will gives large control output and may damage the system. In order to avoid this, the derivative term is ignored and therefore the resulting PI controller is given by,

$$u(t) = K_p e(t) + K_i \int_0^t e(t)dt \tag{8}$$

Where, $u(t)$ is control input, K_p is proportional gain, K_i is integral gain and e(t) is the error signal. Error signal is the difference between Set Point (*SP*) and Measured Variable (*MV*). All the gain parameters must be tuned appropriately so that it will minimize the error signal and give the desired autopilot output.

Various autopilots are designed using SISO design GUI and are explained in subsequent sections. Here design requirements are chosen based on the mission. Apart from this, general design parameters viz. small rise time, settling time, peak overshoot and steady state error also must be satisfied. The time domain specifications achieved by autopilot design considering the gain constraints are also reported below.

3.1 Altitude Hold Autopilot

The altitude is not directly depending on a single state variable, but it depends on more than one variable ($q$and θ) as shown in figure 1. The multi-loop PI altitude hold autopilot is designed using the SISO GUI and the basic aim is to station the airship at desired height. Design requirement in terms of half time ($t_{1/2}$), rise time (t_r) settling time (t_s), peak overshoot ($\%M_p$) and steady state error (e_{ss}) are shown in table 5. Achieved performance specifications using PI controller are shown in figure 2.

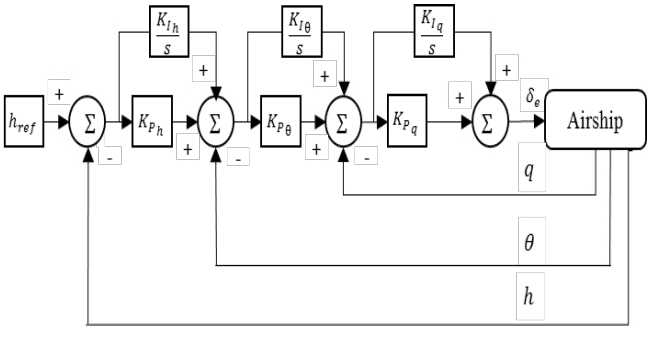

Figure 1. Altitude hold autopilot

Table 5.Design requirements for altitude hold autopilot

Altitude Hold	$t_{1/2}$	t_r	t_p	t_s	e_{ss}
20 km	<200 sec	<200 sec	<200 sec	< 500 sec	±500m

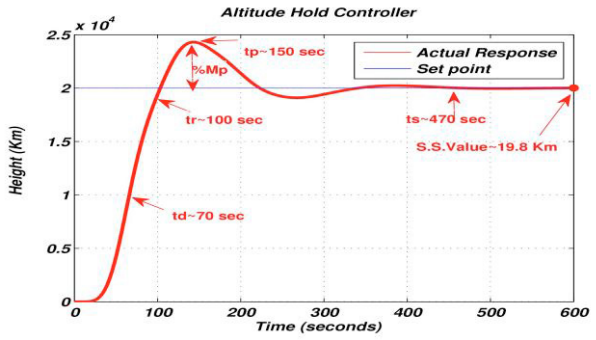

Figure 2. Performance of altitude hold autopilot

3.2 Velocity Hold Autopilot

Velocity hold autopilot has a simple straight forward design as far as the number of loops and variables are considered. Main aim of designing the velocity hold autopilot system is to manoeuvre the airship at constant velocity without any manned control. The control block representing velocity hold autopilot is shown in figure 3. A faster dynamic response is expected since only a single loop is present in the controller design. The design requirements in terms of half time ($t_{1/2}$), rise time (t_r), settling time (t_s), peak overshoot ($\%M_p$) and steady state error (e_{ss}) are chosen approximately and shown in table 6. Achieved performance using controller is shown in figure 4.

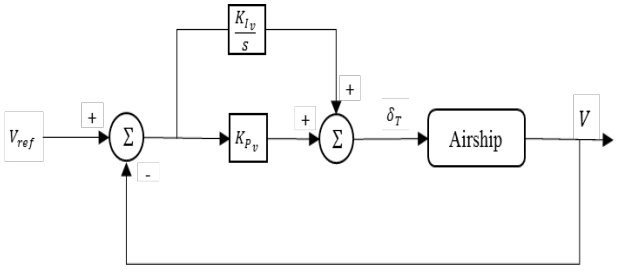

Figure 3. Velocity hold autopilot

Table 6.Design requirements of velocity hold autopilot

Velocity Hold	$t_{1/2}$	t_r	t_p	t_s	e_{ss}
8 m/s	<50 sec	<50 sec	< 50sec	< 100 sec	±0.5m/s

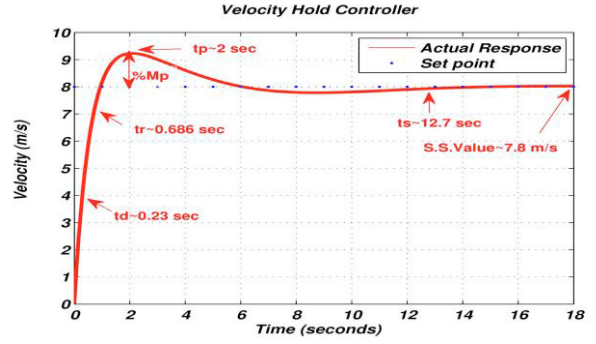

Figure 4. Performance of velocity hold autopilot

3.3 Bank Angle Hold Autopilot

Design of bank angle hold controller is shown in figure 5. Design requirements in terms of half time ($t_{1/2}$), rise time (t_r) settling time (t_s), peak overshoot ($\%M_p$) and steady state error (e_{ss}) are shown in table 7. Achieved optimum performance using controller is shown in figure 6. Here design requirement is chosen based on the fact that the airship is a buoyant vehicles and has larger inertia so it will take some time to respond in the lateral direction. Therefore in case of bank angle tracking, we can expect some sluggish response while it is going to bank at particular angle.

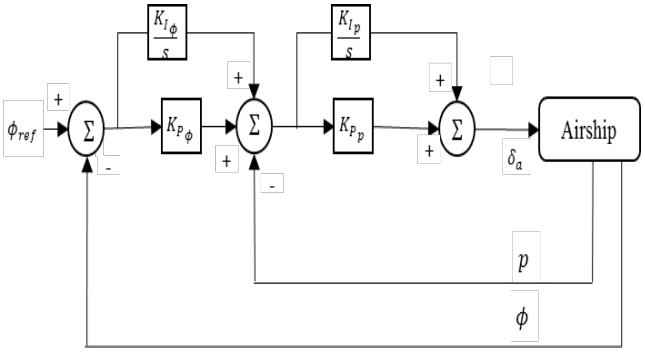

Figure 5. Bank angle hold autopilot

Table 7.Design requirements of bank hold controller

Bank angle Hold	$t_{1/2}$	t_r	M_p	t_s	e_{ss}
0.2 rad	<100 sec	<100 sec	< 25%	< 500 sec	±0.05 rad

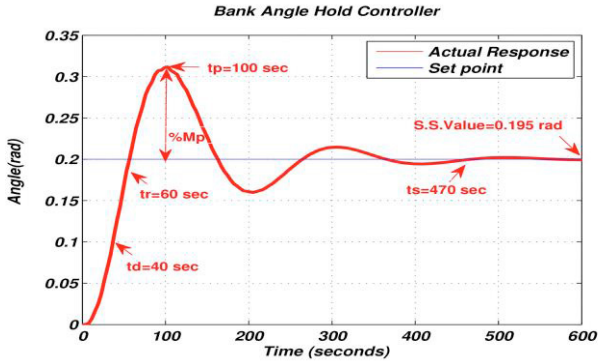

Figure 6. Performance of the bank angle hold autopilot

3.4 Pitch Attitude Hold Autopilot

Pitch attitude hold autopilot is generally implemented for level flight condition. The reference variable is θ and sensor used for feedback is attitude reference gyroscope which generates the error signal proportional to present orientation with respect to desired orientation. Control action will be such that this error should be minimized and desired orientation should be reached quickly. Design of pitch attitude hold autopilot system is shown in the figure 7. Design requirements in terms of half time ($t_{1/2}$), rise time (t_r) settling time (t_s), peak overshoot ($\%M_p$) and steady state error (e_{ss}) are shown in table 8. Achieved performance using controller is shown in figure 8.

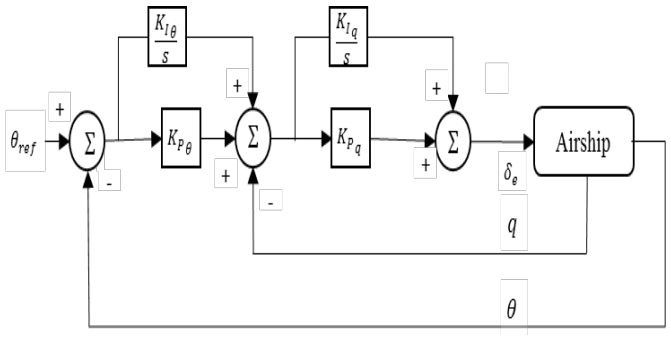

Figure 7. Pitch attitude hold autopilot

Table 8.Design requirements of pitch hold autopilot

Pitch Hold	$t_{1/2}$	t_r	t_s	$\%M_p$	e_{ss}
0.1 rad	<100 sec	<100 sec	<500 sec	< 25%	±0.01 rad

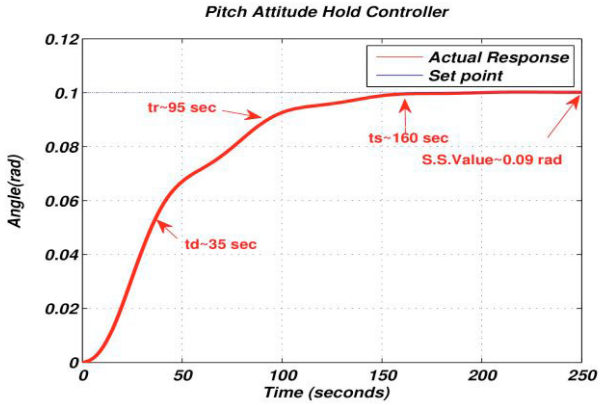

Figure 8. Performance of pitch attitude hold autopilot

All autopilots developed above are giving adequate performance in terms of transient and steady state specifications. Here it is important to note that there is no fixed criteria for the selection of design requirements. Design requirements are approximately fixed based on number of successive loops present in the design and type of mission. Autopilot control system is designed with main objective that it should achieve the required mission parameters with less steady state error and acceptable values of transient specifications.

3.5 Stability Analysis with Autopilots

Apart from the performance and specifications, stability analysis is the most crucial aspect of any control design. Autopilot system can be tuned according to the stability constraints to get better performance. Stability analysis gives an idea about how far the system is from the critical point. This boundary is define by Gain Margin (*GM*) and Phase Margin (*PM*) of the system. The values of *GM* and *PM* of the different autopilots can be obtained using different frequency domain analysis techniques such as Nyquist plot, Bode plots etc. (Stevens,B.L. et al., 1992). Bode diagram for the above mentioned autopilot control systems are shown in the figure 9. Larger values of gain margin and phase margin suggest excellent autopilot design for the system.

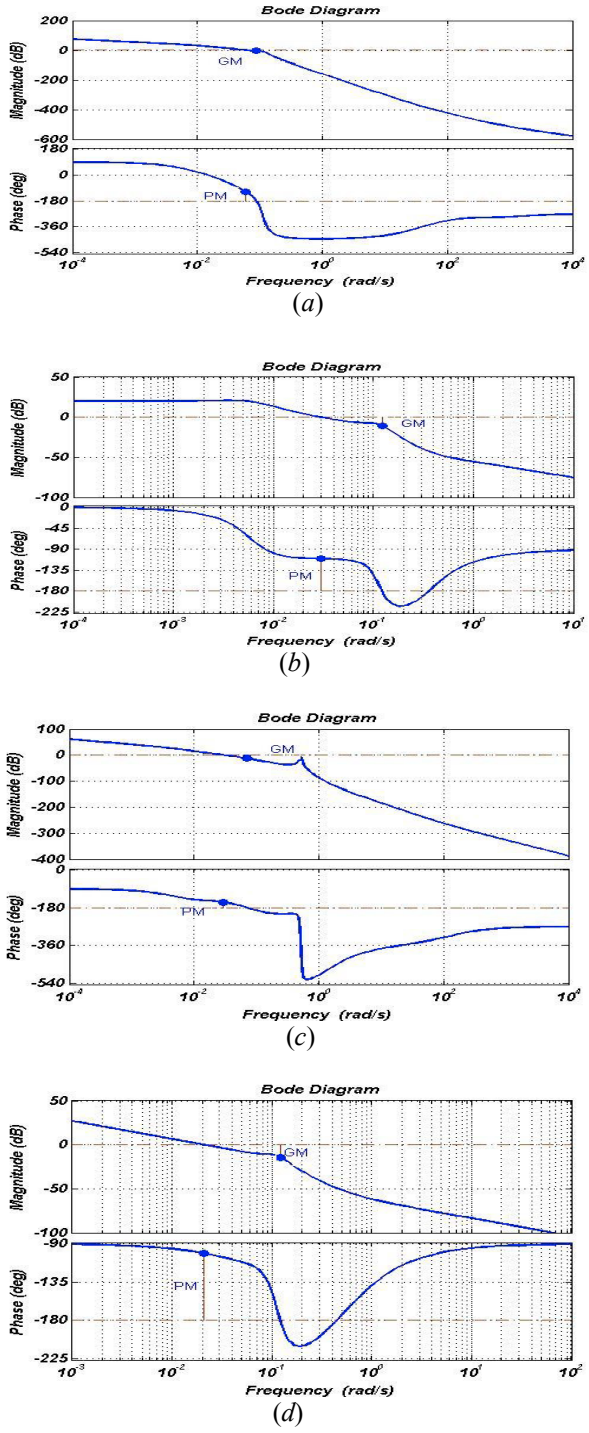

Figure 9.Bode diagram of autopilot system (*a*) Altitude hold (*b*) Velocity hold (*c*) Bank angle hold (*d*) Pitch attitude hold

The obtained values of stability margin of various autopilots are given in table 9. The values of gain margin and phase margin obtained for all the autopilots are positive and hence developed autopilots system results in a stable response. However it can be seen from the values that autopilot design for longitudinal plane (altitude hold, velocity hold and pitch angle hold autopilot) are more challenging than that of lateral plane because of smaller stability margin.

This is due to air speed because air speed plays significant role in longitudinal plane.

Table 9.Stability margins of autopilot system

Stability margin	Autopilots System			
	Altitude Hold	*Velocity Hold*	*Bank Angle Hold*	*Pitch Angle Hold*
GM(db)	4.14	7.4	17.4	14
PM(deg)	60.7	65.6	26.2	76

4. CONCLUSIONS

The overall design architecture of different autopilot systems for the stratospheric airship using PI controller are discussed. All the autopilots except velocity hold autopilot consist inner loops as successive loop closure, therefore slight delay is expected in the transient specification of the dynamic response. However optimum design requirements of all autopilots control system are achieved by perfect tuning of PI gains. As proportional and integral gains have their own individual effects on performance specifications, it is possible that change in one variable affects the dynamic response and may give the undesired result. To avoid this, due consideration is given while tuning the gains. The last section described the stability analysis of designed autopilot for the stratospheric airship. The longitudinal plane autopilots are affected by the airspeed in longitudinal plane and is shown by the lower values of stability margins.

ACKNOWLEDGMENTS

This research is funded and supported by Defence Research and Development Organisation (DRDO), India.The author would like to acknowledge P.Balasubramanian, senior scientist in Defence Research and Development Organisation and Joel, G., Assistant professor in the Department of Aerospace Engineering, IIT Madras for their great supports and encouragement.

REFERENCES

Beard, R. W., and Timothy W. McLain. (2012), "*Small unmanned aircraft: Theory and practice*'', Princeton University Press, New Jersey, USA.

Burgess, C. P. (1927), "*Airship design*'', Ronald Press Company, New York, USA.

How, J. P., Frazzoli, E. and Chowdhary, G. V. (2015). "Linear flight control techniques for unmanned aerial vehicles'', In *Handbook of Unmanned Aerial Vehicles* (pp. 529-576), Springer, Netherlands.

Kadota, H., Kawamura, H., Yamamoto, M., Takaya, T. and Ohuchi, A. (2004), "Vision-based positioning system for indoor blimp robot", 5th IFAC/EURON Symposium on Intelligent Autonomous Vehicles, Instituto Superior Técnico, Lisboa, Portugal.

Khoury, G.A. and Gillett, J.D. (2004), "*Airship Technology*'' Cambridge University Press, New York, USA.

Lee, S. J., Kim, S. P., Kim, T. S., Kim, D. M. and Bang, H. C. (2005), "Design of the Automatic Flight and Guidance Controller for 50m Unmanned Airship Platform'', *International Journal of Aeronautical and Space Sciences*, *6*(2), 64-75.

López Fernández, J., González, P., Sanz, R. and Burgard, W. (2009). "Developing a low-cost autonomous indoor blimp'', *Journal of Physical Agents*, *3*(1), 43-52.

Michael, F., Stephen, M. and Chunjiang, Q. (2007), "The 6-DOF Dynamic Model and Simulation of the Tri-Turbofan Remote-Controlled Airship'' Proceedings of the American Control Conference, 11-13 July, New York, USA.

Stevens, B.L., Lewis, F.L. (1992), "*Aircraft control and simulation*", Wiley inter-science publication, NY, USA.

Vikas, R., Ajit, K., Sinha, N.K., Amitabha, P. and Sati, S.C. (2015), "Configuration Analysis of Stratospheric Airship", Symposium on Applied Aerodynamics and Design of Aerospace Vehicles, VSSC, Thiruvananthapuram, India.

Ziegler, J. G., Nichols, N. B. (1942), "Optimum Settings for Automatic Controllers'', Trans. ASME, Vol. 64, pp.759-76.

APPENDIX

NOTATION

Notation of all the parameter used in the paper are given below.

A_l	Longitudinal plane state transition matrix
B_l	Longitudinal plane control matrix
A_{lt}	Lateral plane state transition matrix
B_{lt}	Lateral plane control matrix
a_x, a_y, a_z	CG coordinates in the body axis system
b_x, b_y, b_z	CB coordinates in body axis system
B	Buoyancy force
J_x, J_y, J_z, J_{xz}	Components of apparent inertia
L_v, L_p, L_r	Rolling moment derivative
M_u, M_w, M_q, M_θ	Pitching moment derivative
m	Airship total mass
m_l	Longitudinal dynamics mass matrix
m_{lt}	Lateral directional mass matrix
m_x, m_y, m_z	Displaced mass in *x*, *y* and *z* direction
N_v, N_P, N_r	Yawing moment derivative
p, q, r	Angular velocity
Q_{lC}	Longitudinal plane controllable matrix
Q_{ltC}	Lateral plane controllable matrix
U	Control input
u, v, w	Linear velocity
$X_{\delta e}, Z_{\delta e}, M_{\delta e}$	Elevator angle stability derivative
X_t, M_t	Thrust stability derivative
X_u, X_w, X_q	Longitudinal derivatives along *X*
$X_{\dot{q}}, Z_{\dot{q}}, M_{\dot{u}}, M_{\dot{w}}$	Derivative expressing virtual mass
Yv, Y_p, Y_r	Lateral derivatives along *Y*
$Y_{\delta_r}, N_{\delta_r}$	Rudder angle stability derivative
$Y_{\dot{v}}, Y_{\dot{p}}, Y_{\dot{r}}, L_{\dot{v}}, L_{\dot{p}}$	Derivatives expressing virtual mass
Z_u, Z_w, Z_q	Longitudinal derivatives along *Z*
ϕ, θ, ψ	Euler angle
δ_e, δ_T	Elevator deflection and thrust
$\delta_r,\ \delta_a$	Rudder and aileron deflection